

# The Origins of the Bulk flow

Richard Watkins<sup>†,1</sup> and Hume A. Feldman<sup>\*,2</sup>

<sup>†</sup>*Department of Physics, Willamette University, Salem, OR 97301, USA.*

<sup>\*</sup>*Department of Physics & Astronomy, University of Kansas, Lawrence, KS 66045, USA.*

emails: <sup>1</sup>[rwatkins@willamette.edu](mailto:rwatkins@willamette.edu); <sup>2</sup>[feldman@ku.edu](mailto:feldman@ku.edu)

29 January 2026

## ABSTRACT

We analyze the origin of the large-scale bulk flow using the CosmicFlows-4 (CF4) peculiar-velocity catalog. We decompose the observed motions into internal components, generated by mass fluctuations within  $200h^{-1}\text{Mpc}$ , and external ones arising from structures beyond this volume. A weighted-average technique is developed to test the model's self-consistency while minimizing the impact of non-Gaussian distance errors. The CF4 velocities show excellent agreement with the predicted internal field, yielding  $\beta = 0.31 \pm 0.01$ . We also determine that the value of the Hubble constant that should be used for calculating peculiar velocities from the CF4 to be  $H_0 = 75.9 \pm 0.1 \text{ km s}^{-1} \text{ Mpc}^{-1}$ , consistent with CF4 calibrations. Using the minimum-variance formalism, we further separate the bulk flow into its internal and external contributions and find that the observed large-scale bulk flow is dominated by sources beyond  $200h^{-1}\text{Mpc}$ . The amplitude of this externally driven flow increases monotonically with scale, consistent with the influence of a distant, massive overdensity. These findings reinforce the reliability of the CF4 velocity field while calling into question the assumption of a spatially uniform flow generated by external sources. Our results challenge the commonly made hypothesis that the flow in our local volume due to external mass concentrations can be modeled as being spatially uniform.

## 1 INTRODUCTION

The study of large-scale peculiar velocities - departures from the uniform Hubble expansion (Hubble 1929) - provides one of the most direct dynamical probes of the large-scale matter distribution in the Universe. On sufficiently large scales, where density perturbations remain in the linear regime, peculiar velocities trace the underlying gravitational potential and thus offer a powerful, independent test of cosmological models (Andernach & Zwicky 2017; Rubin & Ford 1970; Zeldovich & Sunyaev 1980). Averaged over volumes hundreds of Mpc in radius, these motions combine to form what is known as the bulk flow, a coherent motion of the volume, traced by galaxies within it, relative to the cosmic microwave background (CMB) rest frame (e.g. Jacoby et al. 1992; Willick 1994; Strauss & Willick 1995). Many groups have compiled peculiar velocity catalogs (e.g. Rubin & Ford 1970; Rubin et al. 1976; Dressler et al. 1987; Lauer & Postman 1994; Riess et al. 1995; Zaroubi et al. 2001; Kashlinsky et al. 2008; Springob et al. 2014; Tully et al. 2013, 2016) and analyzed them (e.g. Feldman & Watkins 1994; Watkins & Feldman 1995; Nusser & Davis 1995; Feldman & Watkins 1998; Feldman et al. 2003; Hui & Greene 2006; Sarkar et al. 2007; Watkins

& Feldman 2007; Feldman & Watkins 2008; Tully et al. 2008; Abate & Erdođu 2009; Watkins et al. 2009; Feldman et al. 2010; Rathaus et al. 2013; Davis et al. 2011; Nusser & Davis 2011; Nusser et al. 2011; Agarwal et al. 2012; Macaulay et al. 2012; Turnbull et al. 2012; Nusser 2014; Carrick et al. 2015; Watkins & Feldman 2015b,a; Nusser 2016; Hellwing et al. 2017; Peery et al. 2018; Wang et al. 2018) in the past four decades.

In the standard  $\Lambda$ CDM framework (CDM Planck Collaboration et al. 2016), large-scale motions are directly related to the growth of density fluctuations through gravitational instability. The assumptions of homogeneity and isotropy imply that coherent motions should diminish with increasing scale; the standard cosmological model predicts that the root-mean-square amplitude of the bulk flow should be only  $\sim 100 \text{ km s}^{-1}$  for a volume of  $200h^{-1} \text{ Mpc}$ ; however, several observational analyses over the past two decades have reported bulk flows whose amplitudes appear to exceed these expectations (e.g. Kashlinsky et al. 2008; Watkins et al. 2009; Feldman et al. 2010; Ma et al. 2011; Macaulay et al. 2012; Watkins & Feldman 2015a). Such findings, if confirmed, could signal unaccounted-for systematics in peculiar velocity measurements, larger-than-expected density inhomogeneities beyond current survey limits, or even hints of new physics affecting the growth of

structure and the homogeneity of the Universe (e.g. Haslbauer et al. 2020a; Secrest et al. 2022).

The significance of understanding bulk flows extends beyond local dynamics. Measurements of large-scale velocity coherence test the assumptions of statistical isotropy and homogeneity that underpin  $\Lambda$ CDM cosmology. They also provide an independent cross-check of parameters such as the growth rate of structure, the bias factor between galaxies and mass, and the normalization of the matter power spectrum,  $\sigma_8$ . Persistent discrepancies between predicted and observed bulk flows could signal new physics, such as scale-dependent growth, non-trivial dark energy dynamics, or modifications to general relativity on cosmological scales. For an exhaustive discussion of observational evidence for tensions with  $\Lambda$ CDM see Di Valentino et al. (2025).

Recent years have seen significant advances in both data and methodology. The CosmicFlows program (e.g., Tully et al. 2023) now provides distance and velocity information for tens of thousands of galaxies, dramatically expanding the reach and statistical power of peculiar-velocity studies. Simultaneously, improved reconstructions of the local density and velocity fields from redshift surveys (Carrick et al. 2015; Lilow & Nusser 2021; McAlpine et al. 2025); have enabled more robust comparisons between observed velocities and those predicted by the observed matter distribution. Nonetheless, uncertainties remain in the relative contributions of internal flows, driven by structures within the observed volume, and external flows, arising from mass fluctuations beyond the survey boundary. Disentangling these components is essential for identifying the physical origin of the measured bulk flow and for testing the consistency of the  $\Lambda$ CDM paradigm on the largest accessible scales. CF4 allows a detailed comparison between observed and predicted velocity fields, enabling the decomposition of the total flow into internal and external contributions.

In this work, we present a new analysis designed to clarify the origin of the bulk flow reported in Watkins et al. (2023) calculated using the most recent CosmicFlows-4 (CF4, Tully et al. 2023) catalog. They found that the bulk flow in a volume of radius  $200h^{-1}$ Mpc has a magnitude of  $419 \pm 36$  km/s in a direction of Galactic latitude  $b = -8^\circ \pm 4^\circ$  and longitude  $l = 298^\circ \pm 5^\circ$ . They estimated that a bulk flow of this magnitude is in over  $4\sigma$  tension with the standard cosmological model.

Carrick et al. (2015) used matter density information from the 2M++ redshift survey (Lavaux & Hudson 2011) to create a model of the peculiar velocity field originating from mass concentrations within  $200h^{-1}$ Mpc. McAlpine et al. (2025) have recently improved this model using the same redshift data but including simulations and utilizing Bayesian forward modeling. For comparison we will employ both of these models separately. For each model, we use the predicted peculiar velocities to separate the observed peculiar velocities into internal contributions, originating from mass con-

centrations within  $200h^{-1}$  Mpc, and external contributions, originating from beyond this distance, testing the self-consistency of the model through averaged velocity comparisons. This approach mitigates the non-Gaussian effects of distance uncertainties and provides a direct, data-driven way to assess whether the observed flow is compatible with the expected velocity field generated by the local mass distribution.

The remainder of this paper is structured as follows. Section 2 describes the CF4 dataset and our processing of the distance and velocity measurements. Section 3 outlines the theoretical framework used to model internal and external velocity contributions. Section 4 presents our statistical analysis and tests of model consistency, while Section 5 discusses the implications of our results for the origin of the observed bulk flow and for potential deviations from  $\Lambda$ CDM predictions. Section 6 summarizes our conclusions.

## 2 THE COSMICFLOWS4 CATALOG

The CosmicFlows4 (CF4) catalog (Tully et al. 2023) is a compendium of nearly all available cosmological distance measurements. We use the group version of this catalog. It gives distance moduli  $\mu$  with uncertainties  $\sigma_\mu$ , redshift  $cz$ , and location on the sky for over 38,000 galaxies and galaxy groups. Given that the velocity model only applies out to distances of  $200h^{-1}$ Mpc, in this paper we will only use the 23,441 objects with  $cz < 200,000$  km/s from the CF4. Note that we use redshift rather than distance modulus to locate objects in space as it is more accurate, especially for faraway galaxies.

In order to calculate peculiar velocities, we first exponentiate distance moduli to get distances. This process is known to introduce bias into our distances. However, this bias can be calculated and corrected for (see e.g., Watkins & Feldman 2015b). Following Watkins et al. (2023) we calculate corrected distances as

$$d_c = 10^{\frac{\mu}{5} - 5} \exp(-(\kappa\sigma_\mu)^2/2), \quad (1)$$

with uncertainties given by

$$\sigma_c \approx \kappa\sigma_\mu d_c, \quad (2)$$

where  $\kappa = \ln(10)/5$ .

At the distances of objects in the CF4 catalog, deviations from Hubble's law have a significant effect on calculations of peculiar velocities. A common approach is to account for these deviations by using the modified redshift  $z_{mod}$ , calculated as a Taylor series in  $z$ , (see e.g., Visser 2004; Riess et al. 2009; Davis & Scrimgeour 2014; Watkins & Feldman 2015b).

$$z_{mod} = z \left( 1 + \frac{1}{2}(1 - q_o)z - \frac{1}{6}(1 - q_o - 3q_o^2 + j_o)z^2 + \mathcal{O}(z^3) \right), \quad (3)$$

where  $q_o$  is the deceleration parameter,  $j_o$  is the jerk,

and we have assumed a spatially flat Universe. The parameters  $q_o$  and  $j_o$  can be determined empirically (see *e.g.*, Riess et al. 2007; Freire et al. 2017).

The unbiased distances can be used to calculate unbiased peculiar velocities through the formula

$$v_c = (cz_{mod} - H_0 d_c) / (1 + z). \quad (4)$$

We note that while the peculiar velocity estimates given here are unbiased, in that averages over velocities will give the correct result, their probability distributions are skewed and thus nonGaussian. This point warrants further discussion. Velocity estimates are unbiased which tells us that the errors in the velocities will average to zero, even if the distributions of errors is nonGaussian. However, likelihood analyses typically involve the squares of velocity errors. Squaring values that are drawn from a skewed distribution makes their distribution even more skewed and can bias results. Velocities with skewed error distributions can give much different values of  $(v - v_{model})^2$  than velocities with Gaussian errors, even for the same level of uncertainties. While there are velocity estimators that result in Gaussian errors (see Watkins & Feldman 2015b), these estimators are not accurate for all distances. Many researchers choose to work with distance moduli instead of distances or velocities, since distance moduli have Gaussian errors (see *e.g.*, Springob et al. 2016). However, this method involves predicting distance moduli from redshifts and these distance moduli will have non-Gaussian errors due to peculiar velocities.

### 3 THEORY

We begin by assuming that the CF4 peculiar velocities  $v_i$  are the sum of a contribution from the mass distribution inside the region of radius  $200h^{-1}\text{Mpc}$ , which we will call  $v_{int,i}$ , a contribution from the mass distribution outside of this region, which we will call  $v_{ext,i}$ , measurement noise  $\delta_i$ , and an additional contribution  $\delta_{*,i}$  due to galaxies not being perfect tracers of the velocity field. Thus we have

$$v_i = v_{int,i} + v_{ext,i} + \delta_i + \delta_{*,i}. \quad (5)$$

We use the velocity field models of Carrick et al. (2015) and McAlpine et al. (2025) separately to calculate  $v_{int,i}$  for the objects in the CF4 that are within  $200h^{-1}\text{Mpc}$ . We will assume that  $\delta_{*,i}$  are drawn from a Gaussian distribution of width  $\sigma_*$ , which we will take to be 150km/s (see *e.g.*, Turnbull et al. 2012). Gaussian measurement errors in the distance modulus  $\mu$  are translated into non-Gaussian distributed errors when moduli are exponentiated to obtain distance and subsequently velocity errors  $\delta_i$ . However, we can eliminate bias from estimates of  $v_i$ , which ensures that the  $\delta_i$  average to zero (see Sec. 2 above). Note that while it is possible to use a velocity estimator that has Gaussian distributed errors (see, *e.g.*, Watkins & Feldman

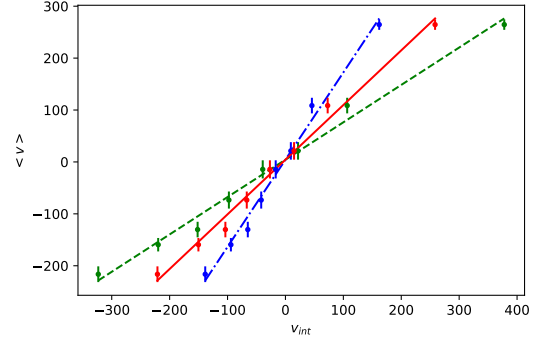


**Figure 1.** Weighted averages of the measured peculiar velocities in bins of  $v_{int}$  from Carrick et al. (2015) for the best fit value of  $H_0$  but varying values of  $\beta$ . Each bin contains 3,000 objects. The blue points and dash-dot slope correspond to  $\beta = 0.43$ , the red points and solid slope correspond to  $\beta = 0.31$  (the best fit value), and the green points and dashed slope correspond to  $\beta = 0.19$ . Velocity of the bin is determined by the weighted average of  $v_{int}$  values of the objects in the bin. The red solid line in the figure has a slope of one.

2015b), these estimators are not accurate at small redshift  $cz$ , which is where much of the information in our data lies.

### 4 TESTING THEORY WITH AVERAGES

As we have discussed above, it is possible to eliminate biases in *averages* even when error distributions are non-Gaussian. Here we will focus on using averages of radial velocities as a tool to study Eq. 5.

As a test of our hypothesis, we average the CF4 velocities in bins based on their values of  $v_{int}$ . Since the other terms in the expression given in Eq. 5 should be uncorrelated with  $v_{int}$ , we should ideally have  $\langle v \rangle = v_{int}$ , where the angle brackets signify an average over the peculiar velocities in an individual  $v_{int}$  bin. Since objects in a given bin have a large range of velocity uncertainties, we do a weighted average over the objects in each bin, using weights  $w_n = (\sigma_n^2 + \sigma_*^2)^{-1}$ , where the index  $n$  references the objects in a particular bin. In order to have similar uncertainties for the averages in each bin, we choose bins to have equal numbers of  $N$  objects. In this paper we used  $N = 3,000$  (the results are fairly independent of this choice). We calculate the  $v_{int}$  value to assign to each bin using a weighted average over the  $v_{int,n}$  values of the objects in the bin using the same weights as for  $\langle v \rangle$ .

Ideally, our averages would fall on a line of slope unity and a  $y$  intercept of zero, indicating the validity of the velocity model given in Eq. 5. There are two parameters that we can adjust in our model to achieve this result.

First, the velocity scale  $\beta = \Omega_m^{0.7}/b$ , where  $\Omega_m$  is the mass density parameter and  $b$  is the bias parameter, determines the growth rate of structure and hence the am-

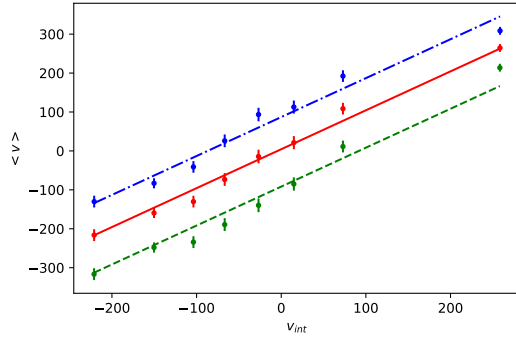


**Figure 2.** Weighted averages of the measured peculiar velocities in bins of  $v_{int}$  from Carrick et al. (2015) for the best fit value of  $\beta$  but varying values of  $H_0$ . Each bin contains 3,000 objects. The green points and dashed slope correspond to  $H_0 = 74\text{km/s/Mpc}$ , the red points and solid line correspond to  $H_0 = 75.8\text{km/s/Mpc}$  (the best fit value), and the blue points and dash-dot slope correspond to  $H_0 = 78\text{km/s/Mpc}$ . Velocity of the bin is determined by the weighted average of  $v_{int}$  values of the objects in the bin. All lines in the figure have a slope of one.

plitude of the internal velocities, (see *e.g.*, Seljak et al. 2005; Davis et al. 2011; Springob et al. 2016). Changing  $\beta$  multiplies the internal velocities by a factor, thus changing the slope of the relationship with the bin averages. This is shown in Fig. 1, where we plot the averages for three different values of  $\beta$ .

Second, we can take the value of the Hubble constant  $H_0$  used to calculate the CF4 velocities to be a free parameter in our analysis. Increasing  $H_0$  adds an amount proportional to distance to all radial velocities, and thus shifts the line of averages upward. Similarly, a decrease in  $H_0$  will shift the line of averages downward. This is shown in Fig. 2, where we plot the averages for three different values of  $H_0$ . Since these two parameters change the line of averages in very different ways they are essentially uncorrelated, and we can determine the best fit values of  $\beta$  and  $H_0$  independently by minimizing the difference between our averages and a line of slope unity and vanishing y-intercept.

Fig. 3 shows the bin averages for the best fit values of  $\beta$  and  $H_0$  with their uncertainties for the internal velocities given by Carrick et al. (2015). The  $v_{int}$  bins contain an equal number of velocities,  $N = 1,000$ . Clearly this matches a line of slope unity well. Our analysis gives  $\beta = 0.31 \pm 0.01$  and  $H_0 = 75.9 \pm 0.1\text{km/s/Mpc}$ . Our value of  $\beta$  is quite consistent with that obtained through a comparison of the 6dF and SDSS surveys to the Carrick et al. (2015) velocities (Said et al. 2020), and our  $H_0$  value is consistent with that determined by the calibration of the CF4 (Tully et al. 2023), with somewhat smaller uncertainties. Note that this estimate of  $H_0$  is specifically the value that should be used with the CF4 to calculate peculiar velocities; our analysis does not in-

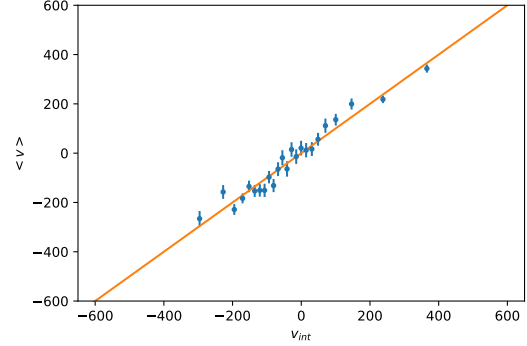


**Figure 3.** Weighted averages of the measured peculiar velocities in bins of  $v_{int}$  from Carrick et al. (2015) with their uncertainties, for the best fit values of  $\beta$  and  $H_0$  and with  $N = 1,000$  objects per bin. The velocity of the bin is determined by the weighted average of  $v_{int}$  values of the objects in the bin. The line in the figure has a slope of one (the same as the red solid line in Fig. 2).

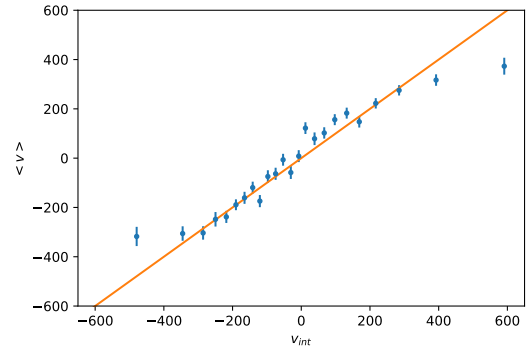


**Figure 4.** Same as Fig. 3 but with data from McAlpine et al. (2025) with best value of  $H_0$  (as mentioned in the text,  $\beta$  is not a parameter that can be adjusted). The line in the figure has a slope of one (the same as the red solid line in Fig. 2).

clude an examination of various systematics that would be necessary in a general estimation of  $H_0$ .

Fig. 4 shows the bin averages for the best fit value of  $H_0$  with their uncertainties for the internal velocities given by McAlpine et al. (2025). Due to their use of simulations, the bias is taken into account implicitly in their calculations and  $\beta$  is not a parameter that can be adjusted. We obtain a best fit value of  $H_0 = 75.84 \pm 0.08\text{km/s}$ , which is in fair agreement with the value obtained using Carrick et al. (2015) velocities. Comparing Fig. 3 and Fig. 4 we note that the McAlpine et al. (2025) model produces a wider range of velocities. While the averages are in good agreement for the smaller velocity bins, we see that the averages underestimate the velocity for the largest velocity bins. Carrick et al. (2015) doesn't give these large velocities and we don't see this effect in their work. We hypothesize that while Carrick et al. (2015) relies on linear theory, the

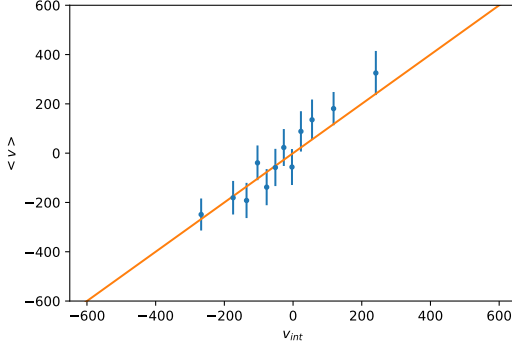


**Figure 5.** Weighted averages of the measured peculiar velocities in bins of  $v_{int}$  from Carrick et al. (2015) and their uncertainties, for objects with  $r > 100h^{-1}\text{Mpc}$  and using the same best fit values of  $\beta$  and  $H_0$  used in Fig. 3 and the same  $N = 1,000$  per bin. Velocity of the bin is determined by the weighted average of  $v_{int}$  values of the objects in the bin. The line in the figure has a slope of one.

model of McAlpine et al. (2025) incorporates nonlinear effects; in particular, the large velocities associated with infall of galaxies into clusters. We are using the groups version of the CF4 catalog, which combines the peculiar velocities of galaxies in a group or cluster to give a single peculiar velocity for that object. Thus we would not expect to see these large galaxy infall velocities in the CF4 data. This explains why averages in these large velocity bins are underestimated.

The value of  $\beta$  we obtain using the Carrick et al. (2015) velocities is quite consistent with that obtained through a comparison of the 6dF and SDSS surveys to the these velocities (Said et al. 2020). The McAlpine et al. (2025) provide a good match with the CF4 bin averages without the need for any scaling. The  $H_0$  value obtained using both models is consistent with that determined by the calibration of the CF4 (Tully et al. 2023), with somewhat smaller uncertainties, and consistent with each other to a high precision. Note that this estimate of  $H_0$  is specifically the value that should be used with the CF4 to calculate peculiar velocities; our analysis does not include an examination of various systematics that would be necessary in a general estimation of  $H_0$ .

One might be concerned that this analysis ignores radial flows in the data, which can mimic variations in the Hubble constant. However, since we weigh by uncertainty, which generally grows with distance, our weighted average are dominated by nearby objects. Since any radial flow must vanish at the origin, it is unlikely that radial flows would have a significant effect on our analysis. A radial flow near our position would also imply that we are at the center of either a void or an overdensity, which is both unlikely and not supported by any observational evidence we are aware of.

In order to test that Eq. 5 holds equally well for

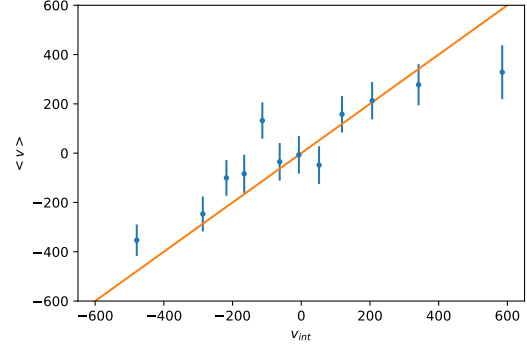


**Figure 6.** Same as Fig. 5 but with data from McAlpine et al. (2025). The line in the figure has a slope of one.

deeper objects, we can institute a minimum distance cutoff  $R_{min}$  and only average only objects beyond the cutoff. In Fig. 5 (Fig. 6) we show the same weighted averages but this time only for objects at distances  $r > 120h^{-1}\text{Mpc}$ . Here we use the same best fit values of  $\beta$  and  $H_0$  as in Fig. 3 (Fig. 4 with only best fit  $H_0$ ). Farther away objects apparently average to the same line as nearby objects, suggesting that radial flows are not having a significant effect on our averages.

Figs. 3 and 5 show a good match between the averages and the  $v_{int}$  bin values for our best fit  $\beta$  and  $H_0$ , thus supporting our velocity model (the same holds for Figs. 4 and 6 with only best fit  $H_0$ ). The level of agreement is particularly striking given that the internal velocities for both Carrick et al. (2015) and McAlpine et al. (2025) were calculated from mass distributions inferred from redshift surveys and the CF4 peculiar velocities were calculated using a combination of redshift and distance estimates. The agreement between them gives us confidence that both methods are accurately estimating velocities, and confirms other studies that make these comparisons using different methods (see e.g., Said et al. (2020); Stiskalek et al. (2025b)).

Our method provides a novel way of measuring  $\beta$  for the CF4 galaxies and the  $H_0$  value that should be used to calculate peculiar velocities for the CF4 very accurately. It is worth noting that the bulk flow calculated in Watkins et al. (2023) does not depend on the value of the  $H_0$  used.

## 5 THE ORIGIN OF THE BULK FLOW

Now that we have validated our model for the CF4 peculiar velocities, we can obtain an estimate for the contribution to peculiar velocities from external sources  $v_{ext,i}$  by subtracting  $v_{int,i}$  from the peculiar velocities  $v_i$ ,

$$v_{ext,i} = v_i - v_{int,i}. \quad (6)$$

Here we consider the bulk flow calculated using the minimum variance (MV) method (Watkins et al. 2009;

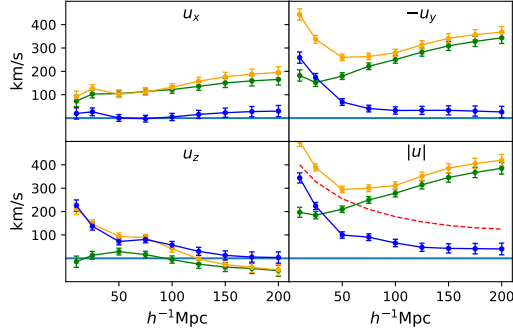


**Figure 7.** The components ( $U_x, -U_y, U_z$ ) of the bulk flow and their magnitude ( $|U|$ ) calculated using the MV method for different radius volumes. The orange line is the total bulk flow. The blue line is contribution to the bulk flow from velocities generated by mass distributions within  $200h^{-1}\text{Mpc}$  from the Carrick et al. (2015) model. The green line is the bulk flow from velocities generated by mass distributions outside of  $200h^{-1}\text{Mpc}$ .

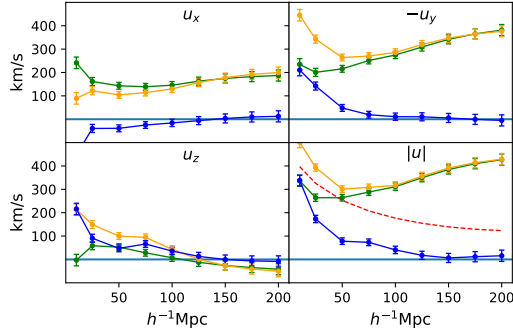


**Figure 8.** Same as Fig. 7 but with data from McAlpine et al. (2025).

Feldman et al. 2010; Watkins & Feldman 2015a; Peery et al. 2018; Watkins et al. 2023). In this formalism the bulk flow is calculated through a weighted average of the peculiar velocities,  $U_j = \sum w_{jk} v_k$ , where  $w_{jk}$  determines the contribution of the velocity of the  $k^{th}$  galaxy to the  $j^{th}$  component of the bulk flow. We can use Eq. 6 to separate out the bulk flow arising from external mass distributions from that due to internal mass distributions;

$$\begin{aligned} U_{ext,j} &= \sum w_{jk} v_{ext,k} \\ U_{int,j} &= \sum w_{jk} v_{int,k} \\ \Rightarrow U_j &= U_{ext,j} + U_{int,j} \end{aligned} \quad (7)$$

In Fig. 7 we show the bulk flow components and magnitudes for the total peculiar velocity as well as for both the contributions from internal (calculated using the Carrick et al. (2015) model) and external sources. Fig. 8 shows the same thing except using the McAlpine

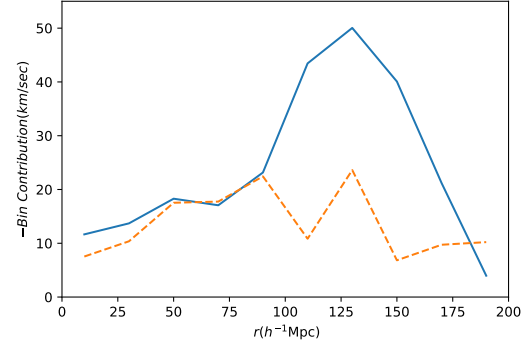


**Figure 9.** The contribution to the bulk flow due to external sources (with the Carrick et al. (2015) model velocities subtracted out) for a sphere of radius  $200h^{-1}\text{Mpc}$  binned in distance and separated into contributions from the hemisphere in the direction of the bulk flow (the blue solid line) and the hemisphere opposite the bulk flow direction (the orange dashed line). We see that the contributions to the bulk flow are largest on the edge of the volume closest to the bulk flow direction, becoming smaller as we move away from the source of the bulk flow.

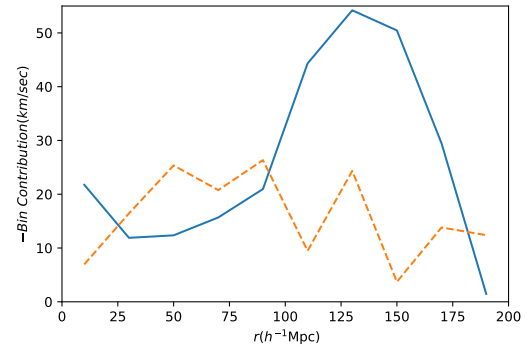


**Figure 10.** Same as Fig. 9 but with data from McAlpine et al. (2025).

et al. (2025) model. What is noteworthy in these figures is that even within a radius as small as  $50h^{-1}\text{Mpc}$ , the bulk flow is dominated by mass distributions located beyond  $200h^{-1}\text{Mpc}$ . This is especially striking given that the influence of the Shapley Concentration (Shapley 1930; Bolejko & Hellaby 2008) is included in  $U_{int,j}$ . The two plots tell essentially the same story, although the McAlpine et al. (2025) model velocities do a slightly better job of having the bulk flow of the volume with a radius of  $200h^{-1}\text{Mpc}$  due to the internal mass concentrations go to zero, since mass concentrations inside of a volume can't cause a bulk motion of that volume.

Figs. 7 and 8 show that the magnitude of the bulk flow from external mass distributions rises monotonically with radius. The most natural explanation for this is the presence of a substantial mass concentration

located in the direction of the bulk flow but lying outside the survey volume. Such a structure would exert its strongest influence near the survey boundary, with the induced flow diminishing toward the Milky Way and beyond. We test this hypothesis by examining the contribution of each galaxy to the externally sourced bulk flow, enabling us to trace the flow pattern throughout the volume.

First, we calculate the contributions to the bulk flow along the direction of the bulk flow for a sphere of radius  $200h^{-1}\text{Mpc}$ . The contribution that the  $k^{\text{th}}$  galaxy's velocity makes to the bulk flow is given by  $\sum_j \hat{U}_j w_{jk} v_{ext,k}$ , where the index  $k$  is not being summed over and  $\hat{U}$  is a unit vector in the direction of the bulk flow. We bin the contributions in distance, separating contributions into those coming from the hemisphere in the direction of the bulk flow and those coming from the hemisphere opposite the bulk flow direction. Note that since we only measure the radial component of a galaxy's velocity, objects with position vectors orthogonal to the bulk flow direction cannot make a contribution to the bulk flow. The result of this calculation for both of our velocity models is shown in Figs. 9 and 10. Consistent with our earlier hypothesis, the contributions to the bulk flow are largest near the edge of the volume in the bulk-flow direction, falling off with increasing distance from that edge. Note that there are no objects beyond  $155h^{-1}\text{Mpc}$  in the direction of the bulk flow, leading to the contribution falling off at the very edge of the volume.

Upon reflection, it seems reasonable that the influence of mass distributions outside the survey volume will be largest at the edges of the survey volume, where they are closest to these mass distributions. However, many papers that attempt to model the velocity field due to external mass distributions model it to be a constant flow over the volume (both Carrick et al. (2015) and McAlpine et al. (2025) do this). This assumption seems to be in conflict with the results presented in this paper. Perhaps even more concerning, this model of a constant flow due to external sources is used in a forward-modeling procedure for calculating Tully-Fisher velocities (Boubel et al. 2024b,a, 2025). It is important to investigate the impact that the constant external flow model has on the results of this kind of analysis, and to develop more accurate models for the velocity field in our volume due to external sources.

## 6 DISCUSSION

Previous work (Watkins et al. 2023) used the CF4 catalog to estimate the bulk flow for a volume of radius  $200h^{-1}\text{Mpc}$  and found it to be in significant tension with the cosmological standard model. In this context, then, it is important to understand the origin of the bulk flow; how much of the bulk flow is from local mass concentrations and how much is caused by sources beyond the survey volume. In this paper, we have com-

pared the CF4 peculiar velocities to the expected velocities  $v_{int}$  given by a model that uses redshift survey information to infer mass concentrations within  $200h^{-1}\text{Mpc}$  volume. By averaging velocities in bins of  $v_{int}$ , we show excellent agreement between the CF4 and both Carrick et al. (2015) and McAlpine et al. (2025) velocities, suggesting that we can accurately separate the contributions to peculiar velocities from local mass distributions from those due to farther away mass concentrations. Our averaging also provides a very precise estimate of the growth factor  $\beta$  and the value of the Hubble constant  $H_0$  that should be used to calculate peculiar velocities from the CF4 distances and redshifts.

Separating the total bulk flow into the sum of a locally sourced bulk flow and a bulk flow from external sources, we find that the observed bulk flow is primarily due to external mass concentrations. We observe the external bulk flow to *increase* with increasing radius out to the limit of the current data. Moreover, by analyzing the contributions to the bulk flow from different regions of the volume, we find that the externally sourced component is strongly non-uniform. The flow is largest in the region closest to the bulk-flow direction and declines steadily with increasing distance from this area.

This is suggestive of a large mass concentration outside the volume in the direction of the bulk flow, and seemingly conflicts with velocities having non-gravitational origins, such as violations of the cosmological principle (see *e.g.*, Böhme et al. (2025); Secret et al. (2022, 2021)) or tilted universe models (Turner 1991, 1992; Kashlinsky et al. 2008; Ma et al. 2011), where we would expect contributions to the bulk flow to be roughly uniform across the volume. There are assertions that suggest that splitting the CMB into half sky maps show variations in  $H_0$  of order of 10%, which may indicate anisotropy in the Universe (see, *e.g.*, Aluri et al. 2022; da Silveira Ferreira et al. 2025). Stiskalek et al. (2026) examine peculiar velocities and do not see a significant anisotropy in  $H_0$ ; however, they use only a fraction of the full CF4 catalog in their analysis.

It is not surprising that external mass concentrations will induce non-uniform flows in the local volume. However, models of the velocity field typically assume that external mass distributions induce a uniform flow in the local volume. The results that we have found here cast doubt on this hypothesis. More work is required to determine the impact of this assumption and to develop more accurate models of the velocity field.

Many questions remain regarding how to reconcile the observed bulk flow with the expectations of the standard cosmological model. Our work showing that the mass concentration responsible for the bulk flow must be further away than  $200h^{-1}\text{Mpc}$  exacerbates the problem, since the further away the mass concentration is, the larger it must be. While the mass concentration required to explain the observed bulk flow is unlikely in the standard model, recent observations by the James Webb telescope (see *e.g.*, Gupta 2023) and studies that suggest the existence of a local (KBC) supervoid (see

e.g., Haslbauer et al. 2020b; Mazurenko et al. 2023; Stiskalek et al. 2025a; Banik & Kalaitzidis 2025) may violate the cosmological principle and challenge  $\Lambda$ CDM and thus affect bulk flow measurements.

More data in the form of deeper redshift surveys and peculiar velocity studies would help clarify the situation. In particular, more data in the direction of the bulk flow is crucial. This region of the sky is close to the galactic plane and relatively understudied.

Ultimately, whether the observed flow represents an extreme, but rare, fluctuation within  $\Lambda$ CDM, an incomplete accounting of the large-scale mass distribution, or a sign of physics beyond the cosmological standard model, remain an open question. Upcoming wide-field surveys and precise distance measurements, particularly in regions currently obscured by the Galactic plane, will be decisive in determining whether the bulk flow marks the limits of cosmic homogeneity or an early harbinger of its breakdown.

**Acknowledgements:** RW was partially supported by NSF grant AST-1907365. HAF was partially supported by NSF grant AST-1907404.

## REFERENCES

Abate A., Erdogdu P., 2009, *MNRAS*, pp 1473–+

Agarwal S., Feldman H. A., Watkins R., 2012, *MNRAS*, 424, 2667

Aluri P. K., et al., 2022, arXiv e-prints, p. arXiv:2207.05765

Andernach H., Zwicky F., 2017, arXiv e-prints, p. arXiv:1711.01693

Banik I., Kalaitzidis V., 2025, *Monthly Notices of the Royal Astronomical Society*, 540, 545

Böhme L., et al., 2025, *Phys. Rev. Lett.*, 135, 201001

Bolejko K., Hellaby C., 2008, *General Relativity and Gravitation*, 40, 1771

Boubel P., Colless M., Said K., Staveley-Smith L., 2024a, *MNRAS*, 531, 84

Boubel P., Colless M., Said K., Staveley-Smith L., 2024b, *MNRAS*, 533, 1550

Boubel P., Colless M., Said K., Staveley-Smith L., 2025, *J. Cosmology Astropart. Phys.*, 2025, 066

Carrick J., Turnbull S. J., Lavaux G., Hudson M. J., 2015, *Monthly Notices of the Royal Astronomical Society*, 450, 317

Davis T. M., Scrimgeour M. I., 2014, *MNRAS*, 442, 1117

Davis M., Nusser A., Masters K. L., Springob C., Huchra J. P., Lemson G., 2011, *MNRAS*, 413, 2906

Di Valentino E., et al., 2025, *Physics of the Dark Universe*, 49, 101965

Dressler A., Faber S. M., Burstein D., Davies R. L., Lynden-Bell D., Terlevich R. J., Wegner G., 1987, *ApJ*, 313, L37

Feldman H. A., Watkins R., 1994, *ApJ*, 430, L17

Feldman H. A., Watkins R., 1998, *ApJ*, 494, L129

Feldman H. A., Watkins R., 2008, *MNRAS*, 387, 825

Feldman H. A., Watkins R., Melott A. L., Chambers S. W., 2003, *ApJ*, 599, 820

Feldman H. A., Watkins R., Hudson M. J., 2010, *MNRAS*, 407, 2328

Freire P. C. C., et al., 2017, *MNRAS*, 471, 857

Gupta R. P., 2023, *MNRAS*, 524, 3385

Haslbauer M., Banik I., Kroupa P., 2020b, *Monthly Notices of the Royal Astronomical Society*, 499, 2845

Haslbauer M., Banik I., Kroupa P., 2020a, *MNRAS*, 499, 2845

Hellwing W. A., Nusser A., Feix M., Bilicki M., 2017, *MNRAS*, 467, 2787

Hubble E., 1929, *Proceedings of the National Academy of Science*, 15, 168

Hui L., Greene P. B., 2006, *Phys. Rev. D*, 73, 123526

Jacoby G. H., et al., 1992, *PASP*, 104, 599

Kashlinsky A., Atrio-Barandela F., Kocevski D., Ebeling H., 2008, *ApJ*, 686, L49

Lauer T. R., Postman M., 1994, *ApJ*, 425, 418

Lavaux G., Hudson M. J., 2011, *Monthly Notices of the Royal Astronomical Society*, 416, 2840

Lilow R., Nusser A., 2021, *MNRAS*, 507, 1557

Ma Y.-Z., Gordon C., Feldman H. A., 2011, *Phys. Rev. D*, 83, 103002

Macaulay E., Feldman H. A., Ferreira P. G., Jaffe A. H., Agarwal S., Hudson M. J., Watkins R., 2012, *MNRAS*, 425, 1709

Mazurenko S., Banik I., Kroupa P., Haslbauer M., 2023, *Monthly Notices of the Royal Astronomical Society*, 527, 4388

McAlpine S., Jasche J., Ata M., Lavaux G., Stiskalek R., Frenk C. S., Jenkins A., 2025, *MNRAS*, 540, 716

Nusser A., 2014, *ApJ*, 795, 3

Nusser A., 2016, *MNRAS*, 455, 178

Nusser A., Davis M., 1995, *MNRAS*, 276, 1391

Nusser A., Davis M., 2011, *ApJ*, 736, 93

Nusser A., Branchini E., Davis M., 2011, *ApJ*, 735, 77

Peery S., Watkins R., Feldman H. A., 2018, *MNRAS*, 481, 1368

Planck Collaboration et al., 2016, *A&A*, 594, A13

Rathaus B., Kovetz E. D., Itzhaki N., 2013, *MNRAS*, 431, 3678

Riess A. G., Press W. H., Kirshner R. P., 1995, *ApJ*, 445, L91

Riess A. G., et al., 2007, *ApJ*, 659, 98

Riess A. G., et al., 2009, *ApJ*, 699, 539

Rubin V. C., Ford Jr. W. K., 1970, *ApJ*, 159, 379

Rubin V. C., Thonnard N., Ford Jr. W. K., Roberts M. S., 1976, *AJ*, 81, 719

Said K., Colless M., Magoulas C., Lucey J. R., Hudson M. J., 2020, *MNRAS*, 497, 1275

Sarkar D., Feldman H. A., Watkins R., 2007, *MNRAS*, 375, 691

Secrest N. J., von Hausegger S., Rameez M., Mohayaee R., Sarkar S., Colin J., 2021, *ApJ*, 908, L51

Secrest N. J., von Hausegger S., Rameez M., Mohayaee R., Sarkar S., 2022, *ApJ*, 937, L31

Seljak U. c. v., et al., 2005, *Phys. Rev. D*, 71, 043511

Shapley H., 1930, Harvard College Observatory Bulletin No. 874, pp. 9–12, 874, 9

Springob C. M., et al., 2014, *MNRAS*, 445, 2677

Springob C. M., et al., 2016, *MNRAS*, 456, 1886

Stiskalek R., Desmond H., Banik I., 2025a, *Monthly Notices of the Royal Astronomical Society*, 543, 1556

Stiskalek R., Desmond H., Devriendt J., Slyz A., Lavaux G., Hudson M. J., Bartlett D. J., Courtois H. M., 2025b, *Monthly Notices of the Royal Astronomical Society*, 545

Stiskalek R., Desmond H., Lavaux G., 2026, *MNRAS*, 546, staf2048

Strauss M. A., Willick J. A., 1995, *Phys. Rep.*, 261, 271

Tully R. B., Shaya E. J., Karachentsev I. D., Courtois H. M., Kocevski D. D., Rizzi L., Peel A., 2008, [ApJ](#), **676**, 184

Tully R. B., et al., 2013, [AJ](#), **146**, 86

Tully R. B., Courtois H. M., Sorce J. G., 2016, [AJ](#), **152**, 50

Tully R. B., et al., 2023, [ApJ](#), **944**, 94

Turnbull S. J., Hudson M. J., Feldman H. A., Hicken M., Kirshner R. P., Watkins R., 2012, [MNRAS](#), **420**, 447

Turner M. S., 1991, [Phys. Rev. D](#), **44**, 3737

Turner M. S., 1992, [General Relativity and Gravitation](#), **24**, 1

Visser M., 2004, [Classical and Quantum Gravity](#), **21**, 2603

Wang Y., Rooney C., Feldman H. A., Watkins R., 2018, [MNRAS](#), **480**, 5332

Watkins R., Feldman H. A., 1995, [ApJ](#), **453**, L73+

Watkins R., Feldman H. A., 2007, [MNRAS](#), **379**, 343

Watkins R., Feldman H. A., 2015a, [MNRAS](#), **447**, 132

Watkins R., Feldman H. A., 2015b, [MNRAS](#), **450**, 1868

Watkins R., Feldman H. A., Hudson M. J., 2009, [MNRAS](#), **392**, 743

Watkins R., et al., 2023, [MNRAS](#), **524**, 1885

Willick J. A., 1994, [ApJS](#), **92**, 1

Zaroubi S., Bernardi M., da Costa L. N., Hoffman Y., Alonso M. V., Wegner G., Willmer C. N. A., Pellegrini P. S., 2001, [MNRAS](#), **326**, 375

Zeldovich Y. B., Sunyaev S. R. A., 1980, [Pisma v Astronomicheskii Zhurnal](#), **6**, 737

da Silveira Ferreira P., Oliveira Ramos R., Ferreira P. S., Cortesi A., Ferrari F., Marra V., Bom C. R., 2025, [arXiv e-prints](#), p. [arXiv:2511.10005](#)